ELSEVIER

Check for updates

Using PhenoCams to track crop phenology and explain the effects of different cropping systems on yield

Yujie Liu [a,*], Christoph Bachofen [a,b], Raphaël Wittwer [c], Gicele Silva Duarte [a], Qing Sun [a], Valentin H. Klaus [a], Nina Buchmann [a]

[a] *Institute of Agricultural Sciences, Department of Environmental Systems Science, ETH Zürich, Universitätstrasse 2, CH-8092 Zürich, Switzerland*
[b] *Plant Ecology Research Laboratory, EPFL, GR B2 417 (Bâtiment GR), Station 2, CH-1015 Lausanne, Switzerland*
[c] *Ecological Farming Group, Agroscope Reckenholz Tänikon, Reckenholzstrasse 191, CH-8046, Zürich, Switzerland*

HIGHLIGHTS

- Cropping system effects on crop phenology are currently unknown but likely to affect yields and thus food security.
- We examined the applicability of PhenoCams for tracking crop phenology and the effects of cropping systems on phenology.
- Crop phenology was significantly affected by cropping systems for both crops studied and linked to yield of winter wheat.
- Organic farming, which changes early growing season conditions, might affect yield via changes in crop phenology.
- PhenoCams are a powerful tool to assess drivers of phenology and yields to potentially increase food security.

GRAPHICAL ABSTRACT
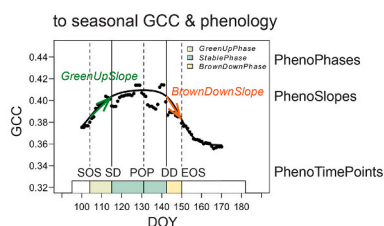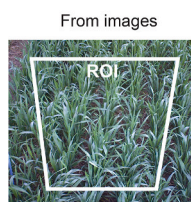
ARTICLE INFO

Editor: Jagadish Timsina

ABSTRACT

CONTEXT: Crop phenology integrates information of how environmental drivers and management practices affect plant performance and crop yield. However, little is known about the impact of cropping systems (CS) on crop phenology and how this relates to differences in yield.

OBJECTIVES: We assessed the applicability of PhenoCams to track crop phenology, how four CS, i.e., organic vs. conventional farming with either intensive or conservation (no/reduced) tillage affect the phenology of a pea-barley mixture and winter wheat, how crop phenology is related to harvest characteristics, e.g., grain yield and total N uptake, and explains CS effects on these characteristics.

METHODS: We used time-lapse cameras (PhenoCams) to track vegetation changes in the two crops and extracted the green chromatic coordinate (GCC) to estimate different phenological metrics, i.e., dates with major changes in GCC (PhenoTimePoints), the duration between those (PhenoPhases), and the rate of increasing or decreasing GCC (PhenoSlopes). We assessed how phenological metrics were affected by different CS, and related phenological metrics to harvest characteristics.

* Corresponding author.
  E-mail address: Yujie.Liu_YL@outlook.com (Y. Liu).

RESULTS AND CONCLUSIONS: CS significantly affected phenological metrics of both crops, with less pronounced effects in the unfertilized pea-barley mixture compared to the fertilized winter wheat, and stronger effects for early-season than for late-season PhenoTimePoints. For winter wheat, organic compared to conventional farming caused an initial growth lag (up to 7 days) and a shorter duration (approximately 10 days) of the period of stable GCC. Winter wheat in reduced/no-tillage systems showed a tendency of delayed phenology (up to 5 days) compared to intensive tillage. While phenological metrics explained harvest characteristics of winter wheat well, they were almost unrelated to those of pea-barley, most likely because pea-barley yields were similar among CS. For winter wheat, effects of CS on harvest characteristics could be well explained by phenological metrics (max. $R^2 = 0.9$). Thus, we demonstrated that delayed phenology acted as an important factor causing lower yield in organic compared to conventional farming.

SIGNIFICANCE: PhenoCams are valuable tool for high-resolution temporal monitoring of crop phenology. As different CS have been proposed as a tool for climate change adaptation, we suggest that the effects of CS on crop phenology need to be considered as they may impact yield via changes in crop phenology, particularly in organic agriculture.

1. Introduction

Phenology, the timing of recurring biological phases, plays a critical role in major ecosystem functions such as water and carbon fluxes (Du et al., 2019; Yao et al., 2017). It drives seasonal soil C dynamics (Hoffmann et al., 2018), determines plant water and nutrient acquisition (Nord and Lynch, 2009), and thus controls gross primary productivity and crop yield (Chen et al., 2019; Liu et al., 2016; Xia et al., 2015). Minor changes in phenology can lead to significant variations in ecosystem productivity (Xia et al., 2015; Yan et al., 2019). For example, the length of the growing season was reported to be positively related to net ecosystem productivity (Baldocchi, 2008; Churkina et al., 2005; Craufurd and Wheeler, 2009). The impact of phenology on plant physiology has been widely studied to understand the ecological responses of vegetation changes to water supply (Estrada-Medina et al., 2013), nutrient conditions (Wang and Tang, 2019), and climate change (Eyshi Rezaei et al., 2017; Macgregor et al., 2019; Piao et al., 2019). How the phenology of crops is affected by agricultural practices is, however, much less understood.

Previous studies on crop phenology focused mostly on tracking changes due to climate change (Craufurd and Wheeler, 2009; Rezaei et al., 2018) or on mapping the large-scale spatial variation of crop phenology (de Castro et al., 2018; Gao and Zhang, 2021), or both (Yang et al., 2020), and were typically based on remote sensing data. As part of regional or global PhenoCam networks, changes in vegetation and phenology of croplands have been monitored, but the drivers of variation in phenology specifically for croplands, such as crop types or management practices, have rarely been addressed (Brown et al., 2016; Richardson et al., 2018a). Management practices at farm or field level can be categorized into distinct agricultural systems (i.e., cropping systems such as organic and conventional farming) and are likely to affect crop phenology. Compared to unmanaged or extensively managed systems such as forests or unfertilized grasslands, the phenology of croplands is rather complex as the relationship between intensive agricultural management and crop phenology is bidirectional. On the one hand, agricultural management practices, including fertilization, pesticide and herbicide applications, are often applied according to a specific crop phenological stage, and are thus guided by phenology. On the other hand, crop phenology is not only determined by environmental factors, but also by management practices, such as sowing date (Klepeckas et al., 2020; Mo et al., 2016), cultivar or genotype choices (Aasen et al., 2020; Eyshi Rezaei et al., 2017; Mo et al., 2016; Rezaei et al., 2018; Schoving et al., 2020) or nitrogen additions (Wang and Tang, 2019). For example, a meta-study showed that phenological changes after nitrogen additions were more pronounced in cropland than in grassland (Wang and Tang, 2019). Therefore, it is necessary to monitor phenology to provide guidance for agricultural management.

To sustainably provide high-quality food from cropland, various management practices have been proposed, including conservation (no/reduced) tillage and the use of cover crops (e.g., Wittwer et al., 2017).

Due to their ecological benefits such as the mitigation of greenhouse gases and carbon sequestration (Gattinger et al., 2012; Huang et al., 2018; Skinner et al., 2019), the preservation of soil fertility (Loaiza Puerta et al., 2018), and the reduction of soil erosion (Seitz et al., 2019), these practices are promising tools to improve the sustainability and performance of cropping systems, e.g., organic and conventional farming. Thus, although extensive research has shown how these practices affect crop yield (Huang et al., 2018; Knapp and van der Heijden, 2018; Pittelkow et al., 2015; Reganold and Wachter, 2016), insight into the impact of different cropping systems on crop phenology and development is still lacking.

Furthermore, looking solely on final yield does not necessarily allow for assessing in-season management interactions with crop development (Verhulst et al., 2011), and thus limits our understanding of the impacts of different management practices. Continuous monitoring of crop growth and development could help to determine in-season crop phenology and to gain mechanistic insights into the consequences of cropping systems on crop growth and development. Digital time-lapse photography with PhenoCams has been widely used to track large-scale vegetation phenology for many ecosystems, e.g., in the Pheno-Cam network (Filippa et al., 2016; Migliavacca et al., 2011; Wingate et al., 2015), to characterize the development of canopy structure such as leaf area index (Garrity et al., 2011; Keenan et al., 2014), to explain temporal changes in CO_2 fluxes (Migliavacca et al., 2011), and to quantify the relationship between phenology and gross primary productivity (Ahrends et al., 2009; Toomey et al., 2015). Traditionally, crop growth dynamics during the growing season were measured by assessing stand harvest characteristics, such as plant height or leaf area index. Despite the ability of PhenoCams to track growth dynamics in cropland (Aasen et al., 2020), to our knowledge, studies using PhenoCams to understand the effect of agricultural practices on crop phenology are still missing. Moreover, the link between crop phenology and crop yield as affected by different cropping systems has not yet been studied in detail, which is limiting our understanding of how cropping systems affect crop performance during the growing season.

Here, we used time-lapse PhenoCams to track crop phenology in a large cropping system experiment, since these cameras are easy-to-use and cost-efficient tools to obtain high resolution temporal information on crop growth. We then assessed how crop phenology is affected by different cropping systems, i.e., organic vs. conventional farming with either intensive or conservation (no/reduced) tillage. We further studied how crop phenology affects different aspects of crop performance at harvest (harvest characteristics), and predicted harvest characteristics using cropping systems and phenological metrics. Assessing not only yield per area, but different harvest characteristics allows for a more comprehensive insight into the effects of cropping systems and phenology on crop performance. To do so, we tested the following hypotheses:

1. PhenoCams can be used to track phenology and extract different phenological metrics for arable crop species.
2. Cropping systems, i.e., organic vs. conventional farming and conservation vs. intensive tillage, influence crop phenology.
3. Crop phenology affects harvest characteristics, such as grain and straw yields, total N uptake, thousand kernel weight (TKW), and ear density.
4. Crop phenology explains the effects of different cropping systems on harvest characteristics.

2. Materials and methods

2.1. Study site and cropping systems

The study site is located at the Swiss Federal Research Station Agroscope Reckenholz near Zurich, Switzerland (47°26′20″N, 8°31′40″S). The long-term average annual temperature is 9.6 °C, the average annual precipitation sums up to 978 mm (1980 to 2019; MeteoSwiss, 2020). Our two-year study utilized a long-term field trial that aims at investigating the productivity and ecological impacts of important arable cropping systems (Farming Systems and Tillage Experiment, FAST; Wittwer et al., 2017). The FAST experiment started in August 2009 and follows a 6-year crop rotation with winter wheat (year 1), maize (year 2), a grain legume crop (year 3), winter wheat (year 4) and a grass-clover mixture (years 5 and 6), representing major crop types for Swiss agriculture. Each year, the respective crops are sown in main plots measuring 6 m × 30 m. The crossed combination of two farming systems (conventional vs. organic) and two levels of tillage intensity (intensive tillage vs. no/reduced tillage) results in four cropping systems, i.e., conventional intensive tillage (C-IT), conventional no-tillage (C-NT), organic intensive tillage (O-IT), organic reduced tillage (O-RT). Reduced tillage, instead of no-tillage, is still applied under organic management as herbicides are prohibited for weed control. The four cropping systems were replicated four times in four blocks with a randomized block design, resulting in 16 plots. This study was conducted in 2018 and 2019, during which a pea-barley mixture (*Pisum sativum* L. and *Hordeum vulgare* L. sown on 26 March 2018, harvested on 16 July 2018) and winter wheat (*Triticum aestivum* sown on 25 October 2018, harvested on 24 July 2019) were grown. The same cultivar for each crop was sowed in all cropping systems. Both crops, pea-barley and winter wheat, are important field crops in Switzerland and beyond, and at the same time differ in functional composition (grass-legume mixture vs. grass monoculture), which makes it particularly valuable to study these two distinct crops.

The soil type of the site is a calcareous Cambisol on glacially deposited Pleistocene sediments, with 23% clay, 34% loam and 43% sand (according to Wittwer et al., 2017). In the conventional systems, mineral fertilizers and herbicides were regularly used, while the organic systems relied only on organic fertilizers and mechanical weed control. None of the studied plots used cover crops. Intensive tillage (IT) was performed with a moldboard plough to a depth of 20 cm in both organic and conventional systems. In the no-tillage management practice of the conventional systems (NT), the soil was not tilled since the beginning of the trial in 2009. Reduced tillage (RT) was performed to a target depth of 5 cm (maximum 10 cm) with a rotary harrow and rototillers.

The pea-barley mixture did not receive any fertilization from sowing to harvest. Fertilization of winter wheat in the conventional managed plots was done with mineral N (nitrogen), as ammonium nitrate (140 kg N ha^{-1} in total), divided into one dose of 60 kg N ha^{-1} on 31 March and two doses of 40 kg N ha^{-1} on 7 April and 27 May 2019. The organic plots were fertilized with a total of 136.4 kg ha^{-1} N, separated into 76.4 kg N ha^{-1} (40 m^3 ha^{-1}) as cattle slurry on 21 March and an equivalent of 60 kg N ha^{-1} as Biorga Quick pellets on 7 April 2019. While the amount of total fertilizer N applied to the crops was similar, timing and dosing differed between organic and conventional cropping systems due to the temporal availability of organic fertilizer and the application of the

national recommendations for fertilization (Richner and Sinaj, 2017). Thus, potential effects of differences in dosing and timing on plant growth are included in the statistical comparison of organic vs. conventional systems.

2.2. Camera installation

We installed time-lapse cameras (TLC 100, Brinno) in all 16 plots to record images of the crops. The cameras were mounted at 1.5 m high on wooden poles that were installed on the south side of the plots, pointing downwards to the crops (60° angle from horizontal) and northwards to the center of each plot. Images were recorded hourly from 24 May (DOY 144) to 11 July (DOY 192) in 2018 for the pea-barley mixture, as well as half-hourly from 5 April (DOY 95) and 10 April (DOY 100) at conventional plots (C-IT and C-NT) and organic plots (O-IT and O-RT), respectively, to 30 June (DOY 181) at all plots in 2019 for winter wheat. According to the automatic mode of the cameras, pictures were taken during daytime but not when it was completely dark. During our study period, this was approximately from 5.00 am to 9.00 pm. For the pea-barely mixture, the camera installation was delayed, thus early phenological data in 2018 is missing. In both years, data recorded by the cameras were downloaded a few days before the respective harvests since cameras had to be taken down due to logistical reasons.

2.3. Image analysis and extraction of the Green Chromatic Coordinate

In total, our PhenoCam dataset was composed of valid observations from 15 plots in the pea-barley mixture and 15 plots in winter wheat. Pictures were missing in one O-RT plot in pea-barley mixture and one C-IT plot in winter wheat due to recording failures. We only used images from 10 Apr (DOY 100) until 21 June (DOY 172) for winter wheat as the cameras were started on different dates, and some of the cameras ran out of batteries earlier than expected. All analyses were performed with the R version 4.0.2 (2020-06-22; R Code Team, 2020).

Image processing and analysis were performed with the R package "Phenopix" (Filippa et al., 2016). First, we determined the region of the image that depicted the crop (region of interest, ROI; Fig. 1) and calculated the Green Chromatic Coordinate (GCC, eq. 1), which is able to efficiently demonstrate a color change of the vegetation by reducing the effect of scene illumination (caused by weather or atmospheric effects, or solar illumination geometry, Richardson et al., 2018a) and can be used with non-calibrated cameras (Sonnentag et al., 2012).

$$GCC = \frac{greenDN}{redDN + greenDN + blueDN} \tag{1}$$

where greenDN, redDN, and blueDN represent the average digital number (DN) of the green, red, and blue channels extracted from the ROI, respectively. To calculate any other CC value (e.g., BCC), the nominator needs to be replaced accordingly.

We excluded nighttime images by excluding images with a brightness (i.e., the sum of redDN, greenDN and blueDN) lower than 85. To exclude images with cloudy or rainy weather conditions, low illumination and dirty lenses, we used a set of filtering processes in a sequence of "*blue, mad, spline, max*" as embedded in the function *AutoFilter*, see Filippa et al. (2016). The "*blue*" filter was designed to remove images with clouds or snow using a threshold on BCC values (Julitta et al., 2014). The "*mad*" filter detects outliers based on the double-differenced time series using the median of absolute deviation about the median (Papale et al., 2006). The "*spline*" filter is based on recursive spline smoothing and residual computation, removing outliers falling outside a given residual envelope (Migliavacca et al., 2011). Finally, we used the "*max*" filter to aggregate GCC values to the daily 90th percentile. Subsequently, a three-day moving average was calculated based on the daily GCC values in order to reduce day-to-day variations, mainly caused by changing illumination under different weather conditions (Hufkens et al., 2012; Sonnentag et al., 2012).
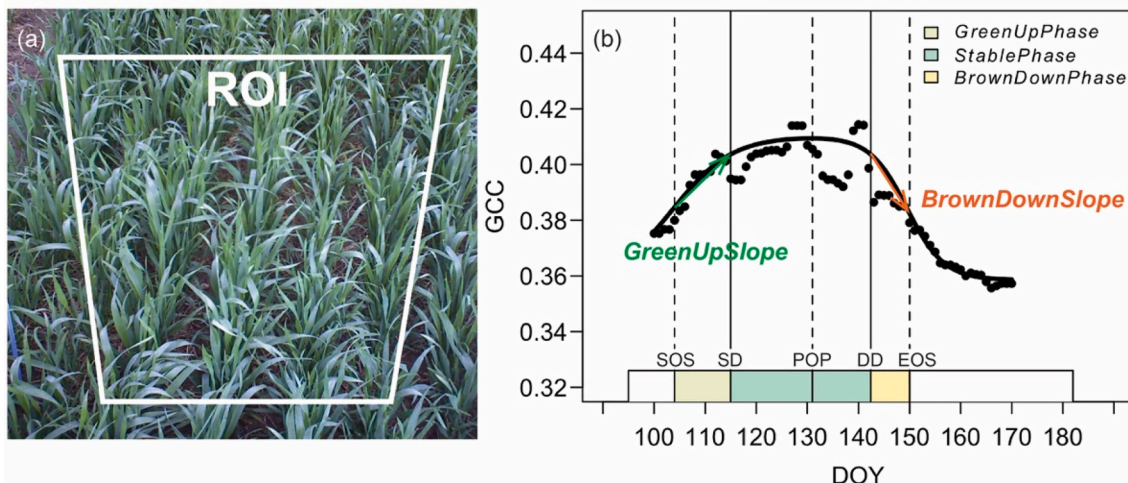
Fig. 1. From PhenoCam pictures (a) to phenology (b). A region of interest (ROI in a) was used to determine daily Green Chromatic Coordinate (GCC) values (black dots in b), to which a double logistic equation (eq. 2 in methods section) was fitted, resulting in a continuous seasonal course of GCC. Phenological metrics were then determined with different methods, either based on the first derivative of the fitted GCC values (dashed vertical lines) or according to the approaches suggested by Gu et al. (solid vertical lines; (Gu et al., 2009). Abbreviations and explanations for all phenological metrics (PhenoTimePoints, PhenoPhases and PhenoSlopes) are given in Table 1.

2.4. Fitting the GCC seasonal course

The GCC signal represents an integrated signal of canopy greenness (Aasen et al., 2020; Keenan et al., 2014; Yang et al., 2014). To capture the GCC seasonal course, we fitted a double logistic regression function per plot to the filtered GCC values (eq. 2) (Beck et al., 2006). The Beck double logistic regression function models the GCC as a function of time (t) using six parameters,

$$GCC(t) = GCC_{min} + (GCC_{max} - GCC_{min})*\left(\frac{1}{e^{(-rsp*(t-SOS))}} + \frac{1}{e^{(-rau*(t-EOS))}}\right)$$
(2)

where GCC_{min} represents the minimum GCC and GCC_{max} represents maximum GCC, SOS (start of season) and EOS (end of season) represent the increasing and decreasing inflection points, and rsp and rau represent the rate of increase or rate of decrease in GCC at SOS and EOS, respectively. In addition, we tested differences in the GCC seasonal courses among the four cropping systems with a repeated measures ANOVA (F-test) by including cropping system as fixed effect, time (DOY) as a random factor and daily GCC values as the response variable in a linear mixed model using the *lmer* function from the package "lme4" (Bates et al., 2015).

2.5. Extraction of phenological metrics

Based on the seasonal GCC curves for each plot in both years, we calculated several phenological metrics from each fitted seasonal curve (Fig. 1, Table 1). A detailed description of all extracted phenological metrics is shown in Table 1. We defined three categories of phenological metrics, i.e., "PhenoTimePoints", "PhenoPhases" and "PhenoSlopes". A "PhenoTimePoint" is a day during the year (DOY) that refers to an event with major changes in GCC. A "PhenoPhase" is a temporal period during the phenological development with a certain duration (Aasen et al., 2020), usually framed by two PhenoTimePoints, while a "PhenoSlope" represents the rate of increase or decrease in GCC during a PhenoPhase. We tested the effect of cropping systems on each of the phenological metrics with the respective linear mixed models, using *lmer* from R package "lme4" (Bates et al., 2015). The cropping system was treated as a fixed effect (four levels), while the experimental block (four levels) was treated as a random effect.

2.6. Stand characteristics

Plant height was measured from the ground to the highest natural point (first leaf or ear) with ten replicates per plot per species, with a folding ruler. It was measured during sunny and non-windy days at noon four times between 22 May and 9 July 2018 for the pea-barley mixture, and six times between 6 Mar and 27 June 2019 for winter wheat. Ten plants within the central region (1 m × 1.5 m) of each plot were chosen randomly for these height measurements. The Leaf Area Index (LAI; m^2 m^{-2}) measurements consisted of one measurement above the canopy, followed by nine measurements below the canopy at ground height (replicated three times during each measurement) at regular intervals during 23 April and 25 June 2019 using a LAI-2000 (Li-Cor, Logan, UT, USA), also within the central region. LAI was measured for winter wheat only. Additionally, the Normalized Different Vegetation Index (NDVI) was computed from aerial images taken with a multispectral camera (Parrot Sequoia, Parrot SA, Paris) capturing Green (550 nm), Red (660 nm), Red Edge (735 nm) and Near Infrared (790 nm) reflectance values, mounted on an autonomous unmanned aerial vehicle (eBee, SenseFly, Parrot SA, Paris). Five flights were carried out between 20 April and 10 July 2018 for the pea-barley mixture, and five flights between 22 March and 4 June 2019 for winter wheat, at an average ground resolution of 5 cm per pixel. Additional to camera setting calibrations, a sunshine sensor (Parrot Sequoia) and a reflectance panel were used for radiometric calibration of the pictures during image processing with the software Pix4Dmapper (Pix4D SA, Prilly). For each flight, reflectance maps for each band were generated and an NDVI map calculated (eq. 3) as:

$$NDVI = (NIR - Red)/(NIR + Red)$$
(3)

where NIR and Red are the reflectance values at 790 nm and 660 nm, respectively. NDVI values at the plot level were then extracted as mean pixel values from the inner 50% area of each plot.

To compare the seasonal dynamics of GCC, NDVI and other stand characteristics qualitatively, we normalized their values (χ_0) relative to their minimum and maximum values (χ_{max} and χ_{min}) over the growing season for each individual plot (eq. 4).

$$\mathscr{X}_{norm} = \frac{\chi_0 - \chi_{min}}{\chi_{max} - \chi_{min}}$$
(4)

where χ_0 refers to NDVI, LAI, plant height or daily means of fitted GCC

Table 1
Phenological metrics used in this study with their abbreviations, calculation method and related references.

Abbreviation	Name of feature	Calculation methods	Methods and references
(1) PhenoTimePoints			
SOS	Start of growing season (green up)	The date when GCC'(t) was largest	Derivative method (Filippa et al., 2016)
SD	Stabilization date	Based on a combination of local maxima in the first derivative, the intersection between recovery line and maxline defines the reaching of the plateau	Gu method (Gu et al., 2009), adapted by (Filippa et al., 2016)
POP	Position of peak greenness	The date of maximum GCC of the fitted GCC curves	Derivative method (Filippa et al., 2016)
DD	Downturn date	Based on a combination of local maxima in the first derivative, the intersection between the plateau line and the senescence line	Gu method (Gu et al., 2009), adapted by (Filippa et al., 2016)
EOS	End of season	The date when GCC'(t) was at the minimum	Derivative method (Filippa et al., 2016)
(2) PhenoPhases			
GreenUpPhase	Period of ascending GCC	Length of phase between SOS and SD	Gu method (Gu et al., 2009), adapted by (Filippa et al., 2016)
StablePhase	Period with relatively stable GCC	Length of phase between SD and DD, refers to a relatively steady stage of crop development in the middle of the growing season	Derivative method (Filippa et al., 2016)
BrownDownPhase	Period with descending GCC	Length of phase between DD and EOS	This study
LOS	Length of growing season	Length of phase between SOS and EOS	This study
(3) PhenoSlopes			
GreenUpSlope	Slope of ascending GCC during *GreenUpPhase*	The linear slope of GCC between the day of SOS and SD, represented by times 10,000	This study
BrownDownSlope	Slope of descending GCC during *BrownDownPhase*	The linear slope of GCC between the day of POP and EOS, represented by times 10,000	This study

for each plot.

2.7. Harvest characteristics and their relation to phenology and cropping systems

Aboveground biomass was collected within two 0.25 m^2 areas that contains three rows of crops per plot by cutting the plants 1 cm above the ground on 16 July 2018 for pea-barley mixture and 24 July 2019 for winter wheat. After drying grains and straws at 60 °C until constant weight, grain yield and straw yield (t/ha of 100% dry matter) were recorded separately. Yield was calculated by transferring the weight of two 0.25 m^2 areas per plot to tons per hectare (t/ha). The thousand kernel weight (TKW; given in g/1000) was calculated by weighing 100 randomly selected grains or peas, respectively. Ear density (ears/m^2) was estimated by counting the number of wheat and barley ears or pea plants per m^2 in the harvested areas. N concentration (N%; g/kg of dry matter) in grain and straw was measured using an elemental analyzer (Euro EA, HEKAtech, Wegberg). Total N uptake (kg N/ha) was calculated according to eq. 5:

$$Total\ N\ uptake = N\%_{grain} \times grain\ yields + N\%_{straw} \times straw\ yields \quad (5)$$

where $N\%_{grain}$ and $N\%_{straw}$ represent N concentrations in grain and straw, respectively.

For both crops, we analyzed how each harvest characteristic is affected by cropping system with separate linear mixed models. Cropping system was a fixed effect, and the experimental block was a random effect. For winter wheat only, to evaluate the relevance of phenology for crop performance at harvest, we first explored the relations between the harvest characteristics (i.e., grain yield, straw yield, total N uptake, TKW and ear density) and the phenological metrics with the Pearson correlation coefficient (*Pearson's r*). Second, to analyze the combined effects of multiple phenological metrics on harvesting characteristics, we selected the phenological metrics that showed a significant correlation with the harvest characteristics (from the last step) and included them in multiple regression models for each of the harvest characteristics. To determine the most influential phenological metrics, we performed a stepwise model selection based on the Akaike information criterion (AIC). The thereby selected phenological metrics were included in a multiple regression model together with the cropping systems to

perform variance partitioning and disentangle the combined effects of cropping system and phenology on harvest characteristics. Third, as *varpart* allows for a maximum of four explanatory variables, cropping system for sure needs to be considered as a variable, which means three phenological metrics at most can be used for variance participating. In cases where more than three phenological metrics were included in the multiple regression models from the last step, we conducted another model selection prior to the variance partitioning, using the *regsubsets* function from the R package "leaps" to select the three best predictors with the highest explanatory power to explain harvest characteristics (Lumley, 2020). This was, however, only done when more than three phenological metrics were significantly related to harvest characteristics (i.e., total N uptake, ear density). Last, we used *varpart* from the R package "Vegan" (Oksanen et al., 2020), which partitions the variation in the response variable (i.e., harvest characteristics) into components accounted for by up to four explanatory variables, i.e., cropping systems and no more than three phenological metrics (selected from last step).

3. Results

3.1. Phenology across different cropping systems

3.1.1. Seasonal GCC courses of the two crops

The phenology could be continuously tracked with GCC from late spring for pea-barley mixture and from early spring for winter wheat throughout the growing season until crop senescence/ripening set in before the respective harvests (Fig. 2). The pea-barley mixture reached its maximum GCC value (POP, i.e., position of peak greenness) around DOY 150 (except for C-NT) and stayed at relatively high values (up to 0.4) rather long (until around DOY 170, the DD, i.e., Downturn Date), before decreasing relatively fast. Low GCC values (of around 0.34 after DOY 185) were reached during ripening, prior to harvest.

A slightly different course of the GCC-based phenology was observed for winter wheat (Fig. 2b). Here, GCC values increased gradually from low values of the overwintering plants (0.37 for C-NT and O-RT and 0.38 for C-IT and O-IT at DOY 100) and reached their maxima (POP; at DOY 130) relatively fast (within 30 days). Both organic cropping systems (O-IT and O-RT) showed a relatively short period with outstanding high GCC values (*StablePhase*; period between SD and DD, i.e., between Stabilisation Date and Downturn Date) in the middle of the growing season
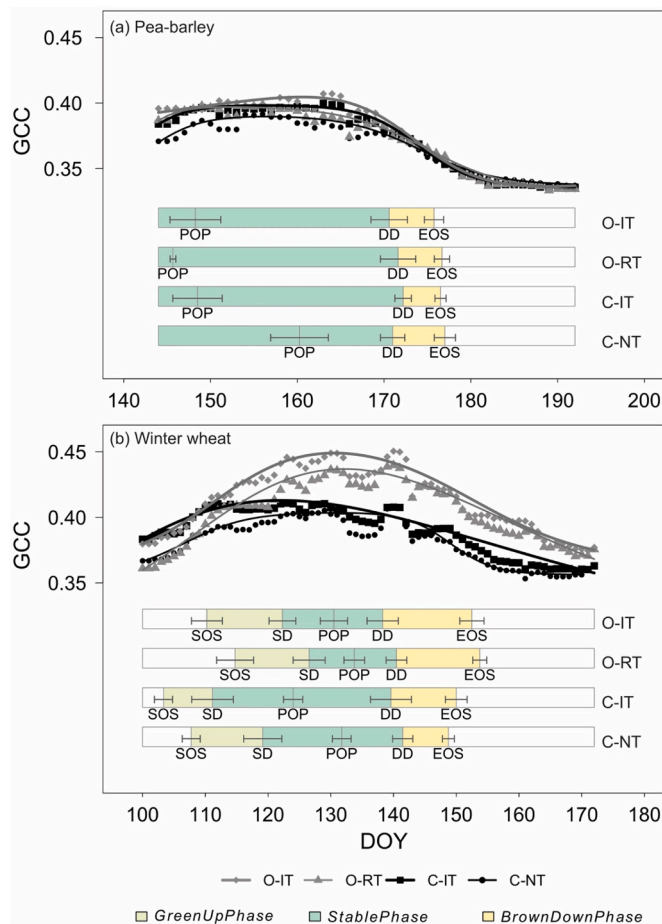
Fig. 2. Seasonal course (dots and curves) of Green Chromatic Coordinate (GCC) and phenological metrics of cropping systems for (a) pea-barley mixture and (b) winter wheat. Curves were fitted to the daily mean GCC values of each cropping system (i.e., the average of the replicated plots in four blocks). Different symbols indicate the four cropping systems. Start and end of each box represent the measurement periods during the two years, with a later start for pea-barley mixture in 2018. Phenological metrics are shown as means and standard errors of PhenoTimepoints. PhenoPhases are shown with different colors. Abbreviations and explanations for all phenological metrics are given in Table 1. Cropping systems are conventional intensive tillage (C-IT), conventional no-tillage (C-NT), organic intensive tillage (O-IT) and organic reduced tillage (O-RT). Statistical results for effects of cropping systems on each single phenological metric are given in Table 2. Please note that the range of the x-axes differs for the two panels.

(up to 0.45). The *StablePhase* for both conventional cropping systems (C-IT and C-NT) was longer and characterised by lower GCC values (up to 0.41). For all cropping systems, GCC values then steadily decreased, reaching low, stable GCC values (around 0.36 at DOY 170) during ripening, prior to harvest.

3.1.2. Effect of cropping systems on phenological metrics

The phenology, represented by seasonal GCC courses, of pea-barley mixture as well as winter wheat were significantly different among cropping systems (repeated measures ANOVA, pea-barley mixture: $F = 23.42$, $P < 0.001$; winter wheat: $F = 552.79$, $P < 0.001$). Not only the seasonal course of GCC values differed among the cropping systems, but also many of the phenological metrics derived from the curves differed (Table 2). In pea-barley, POP was earliest in O-RT (DOY 145.7), followed by O-IT and C-IT (DOY 148.4 and 148.5; respectively), and significantly later in C-NT (DOY 160.3). No effects of cropping systems in the pea-barley mixture were detectable on the *BrownDownPhase* and its associated DD and EOS (End of Season) dates. Much in contrast, in winter

wheat, cropping systems particularly affected the early season Pheno-TimePoints, i.e., SOS, SD, and POP, while the late season PhenoTime-Points, i.e., DD and EOS, were again unaffected. Noticeably, winter wheat grown under intensive tillage (C-IT and O-IT) had an earlier growth compared to those managed under no/reduced tillage (C-NT and O-RT), indicated by relatively early dates of SOS, SD and POP, in both conventional and organic systems. For example, SOS was earliest in C-IT (DOY 103.3), followed by C-NT and O-IT (DOY 107.8 and 110.3; respectively), and latest in O-RT (DOY 114.8), while POP was earliest in C-IT (DOY 124), followed by O-IT, C-NT and O-RT (DOY 130.5, 131.8 and 133.9; respectively). This resulted in an almost two times longer *StablePhase* for winter wheat in the two conventional systems (22 to 28 days) than those in two organic systems (13 to 14 days). Subsequently, with relative early dates of DD and late dates of EOS, both organic systems completed the growing season with a significantly longer *BrownDownPhase* (13 to 14 days) compared to the two conventional systems (7 to 10 days; Table 2). Additionally, the *BrownDownSlope* was steepest in C-IT (−5.3), indicating the slowest decrease in GCC toward ripening, followed by C-NT (−14.3) and O-IT (−20.4)), and slowest in O-RT (−27.3). In contrast, no cropping system effects were found on *GreenUpSlope* and *LOS*, suggesting that the increase in GCC before its peak was irrespective of cropping systems (Fig. 2b, Table 2).

3.1.3. Relationships between phenology and stand characteristics

We observed similar seasonal dynamics for GCC and NDVI in both crops (Fig. 3), with NDVI slightly lagging behind GCC (by about 10 days). Moreover, while GCC and NDVI showed pronounced maxima and decreased towards the end of the growing season, crop height of all crop species increased until after the GCC and NDVI maxima and stayed high until harvest. Crop height maximums occurred near the date of DD in pea-barley mixture (Fig. 3a) and even after EOS in winter wheat (DOY 151; Fig. 3b). Moreover, GCC peaked much earlier than stand LAI and crop height for winter wheat (Fig. 3b). LAI was still very low (10% of its maximum value) during the *GreenUpPhase* before rapidly increasing during the *StablePhase* (SD at DOY 120), reaching its maximum shortly after the end of the *StablePhase* (DD at DOY 140). When GCC peaked at DOY 130, LAI had reached 76% of its maximum value, while height was only at 45% of its maximum. LAI remained stable throughout the *BrownDownPhase* (EOS at DOY 151), only decreasing very late as crop ripening/senescence approached (Fig. 3b). These findings also held true when assessed for each cropping system separately (Fig. S1).

3.2. Harvest characteristics

3.2.1. Effects of cropping systems on harvest characteristics

For pea-barley mixture, only ear density was affected by cropping systems, while all other harvest characteristics such as total grain and straw yield, total N uptake, and TKW were not affected by cropping systems. The highest ear density was achieved in O-IT (approximately 235 per m²), compared to those in other cropping systems (between 130 and 151 per m²). In winter wheat, on the other hand, all five harvest characteristics were significantly affected by cropping systems. Grain yield (on average 5.7 t/ha) were highest in C-IT, intermediate in C-NT and O-IT, and lowest in O-RT. Even more pronounced were the differences for straw yield, which were 25% higher in the two conventional systems (8 to 8.2 t/ha) than in two organic systems (5.7 to 6.4 t/ha). Similar to straw yield, total N uptake (on average 172 kg N/ha) was 47% higher in conventional systems than in organic systems. In contrast, TKW (on average 39 g/1000 grain) was 7.6% higher in organic than in conventional systems. In case of ear density, we observed highest numbers in the two conventional systems (on average 272 ears/m²), intermediate numbers in O-IT (213 ears/m², and lowest ear density in O-RT (178 ears/m², Table 2).

3.2.2. Effects of phenology on harvest characteristics

In general, phenological metrics were more strongly correlated with

Table 2

Effects of cropping systems on phenological metrics and harvest characteristics in pea-barley mixture and winter wheat. Mean values and standard errors of phenological metrics and harvest characteristics for each cropping system are shown. Asterisks indicate significant effects of cropping systems: *** $P < 0.001$, ** $0.001 \leq P < 0.01$, * $0.01 \leq P < 0.05$ according to linear mixed models. Significant effects of cropping systems are given in bold ($P < 0.05$), with letters indicating significant differences among cropping systems derived from Tukey post-hoc tests ($P < 0.05$, n = 16 for pea-barley mixture and winter wheat respectively for harvest characteristics; n = 15 for pea-barley mixture and winter wheat respectively for phenological metrics). Cropping systems are conventional intensive tillage (C-IT), conventional reduced tillage (C-NT), organic intensive tillage (O-IT) and organic reduced tillage (O-RT). Abbreviations for phenological metrics: see Table 1. *NA* = not available due to missing data.

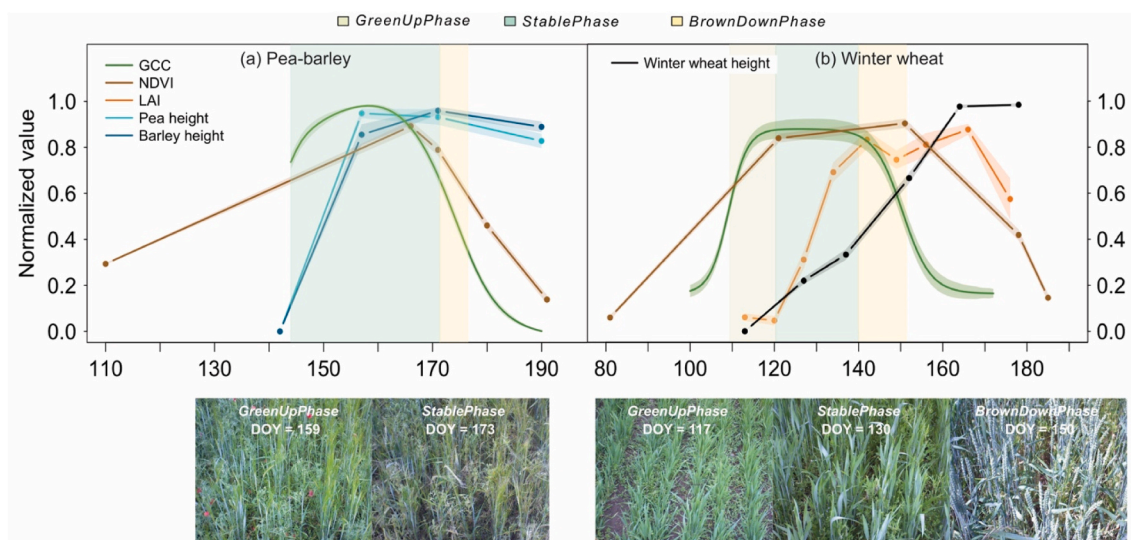|	Pea-barley mixture					Winter wheat				
	F	C-IT	C-NT	O-IT	O-RT	*F*	C-IT	C-NT	O-IT	O-RT
PhenoTimePoints (DOY)										
SOS	*NA*	*NA*	*NA*	*NA*	*NA*	4.07*	103.3 ± 1.5a	107.8 ± 1.4ab	110.3 ± 2.5ab	114.8 ± 3.0b
SD	*NA*	*NA*	*NA*	*NA*	*NA*	5.06*	111.2 ± 3.3a	119.2 ± 3.0ab	122.3 ± 4.3b	126.6 ± 2.6b
POP	**25.70*****	**148.5 ± 2.8a**	**160.3 ± 3.3b**	**148.3 ± 2.9a**	**145.7 ± 0.3a**	4.92*	124.0 ± 1.5a	131.8 ± 1.5b	130.5 ± 2.2b	133.8 ± 1.7b
DD	0.21	172.2 ± 0.9	171.0 ± 1.4	170.6 ± 2.1	171.6 ± 2.0	0.40	139.6 ± 3.3	141.5 ± 1.6	138.3 ± 2.5	140.5 ± 1.7
EOS	0.35	176.5 ± 0.7	177.0 ± 1.2	175.8 ± 1.1	176.7 ± 0.9	2.77	150.0 ± 1.7	148.8 ± 0.9	152.5 ± 1.9	153.8 ± 1.1
PhenoPhases (days)										
GreenUpPhase	*NA*	*NA*	*NA*	*NA*	*NA*	1.09	7.8 ± 3.1	11.4 ± 2.1	12.0 ± 0.7	11.8 ± 0.8
StablePhase	*NA*	*NA*	*NA*	*NA*	*NA*	3.61*	28.4 ± 6.4ab	22.3 ± 3.9a	16.0 ± 0.8b	13.9 ± 1.2b
BrownDownPhase	0.73	4.3 ± 0.5	6.0 ± 0.7	5.2 ± 1.0	5.1 ± 1.2	3.81*	10.4 ± 1.9ab	7.3 ± 0.7a	14.2 ± 1.5b	13.3 ± 2.1b
LOS	*NA*	*NA*	*NA*	*NA*	*NA*	1.35	46.7 ± 2.7	41.0 ± 1.9	42.3 ± 2.1	39.0 ± 3.8
PhenoSlopes										
GreenUpSlope	*NA*	*NA*	*NA*	*NA*	*NA*	0.55	18.9 ± 13.3	12.2 ± 2.4	23.6 ± 4.6	16.5 ± 5.8
BrownDownSlope	2.58	- 21.5 ± 8.3	- 19.6 ± 7.2	−44.8 ± 9.5	−20.2 ± 6.6	7.65*	−5.3 ± 2.1b	−14.3 ± 5.1ab	−20.4 ± 4.1ab	−27.3 ± 4.6a
Harvest characteristics										
Grain yield (t/ha)	2.42	4.35 ± 0.60	3.50 ± 0.31	3.92 ± 0.38	3.25 ± 0.18	**6.84*****	**6.55 ± 0.15c**	**6.15 ± 0.37bc**	**5.35 ± 0.52bc**	**4.60 ± 0.52a**
Straw yield (t/ha)	2.73	3.08 ± 0.40	2.48 ± 0.17	2.95 ± 0.25	2.45 ± 0.05	**7.31 ****	**8.00 ± 0.36b**	**8.20 ± 0.39b**	**6.55 ± 0.75a**	**5.73 ± 0.50a**
Total N uptake (kg N /ha)	1.47	164.50 ± 22.50	139.75 ± 12.86	141.25 ± 18.09	124.00 ± 7.47	**24.12****	**219.75 ± 13.22b**	**225.50 ± 14.77b**	**137.25 ± 20.86a**	**108.25 ± 15.39a**
TKW (g/1000 grain)	1.53	273.58 ± 5.50	294.34 ± 7.50	281.29 ± 8.40	277.64 ± 7.30	**7.54****	**38.15 ± 0.45a**	**37.29 ± 0.99a**	**40.24 ± 0.66b**	**41.05 ± 0.87b**
Ear density (ears/m²)	**5.91***	**151.25 ± 25.22a**	**130.00 ± 18.97a**	**235.00 ± 34.65b**	**136.00 ± 16.86a**	**19.67*****	**265.75 ± 9.59c**	**278.25 ± 9.41c**	**212.75 ± 15.96b**	**178.25 ± 14.64a**

Fig. 3. Seasonal courses of Green Chromatic Coordinate (GCC) and NDVI in relation to further stand characteristics, i.e., LAI and plant height in (a) pea-barley mixture and (b) winter wheat. For comparability, all measurements were normalized to range from 0 to 1. Solid lines indicate mean values of each variable averaged over all plots (for GCC: n = 15 for pea-barley mixture and winter wheat each; for all other variables: n = 16 for both crops). Shaded areas around the lines represent standard errors. Underlying colors indicate PhenoPhases (as defined in Fig. 2). Please note that the range of the x-axes differs for the two panels. PhenoCam images displayed below the panels were taken from the same plot, managed organically with intensive tillage (O-IT).

harvest characteristics in winter wheat than in the pea-barley mixture (Fig. 5). In the pea-barley mixture, the *BrownDownSlope* correlated significantly with total N uptake (*Pearson's r* = 0.52), indicating that a slower rate of descending GCC was related to higher N uptake. Because smaller (more negative values) of *BrownDownSlope* depict a steeper decrease of the GCC curves, this positive correlation indicated that the higher the N uptake, the flatter the decrease in GCC between DD and EOS. However, all other phenological metrics showed no significant correlation with any harvest characteristics of the pea-barley mixture (−0.35 < *Pearson's r* < 0.39). When analysing the harvest characteristics for pea and barley separately, *BrownDownSlope* was found to be positively correlated with grain yield, straw yield and total N uptake of pea (*Pearson's r* > 0.55, Fig. S2). However, none of the phenological metrics correlated with any harvest characteristics of barley (Fig. S2).

Much in contrast, grain and straw yields as well as total N uptake and ear density of winter wheat were negatively correlated to SOS, SD, POP and EOS (*Pearson's r* < −0.59), and positively correlated with the length of the *StablePhase*, and *BrownDownSlope* (*Pearson's r* > 0.60). Specifically, harvest characteristics decreased the most with SOS and SD, thus the later the season started, the later GCC peaked, and the shorter the StablePhase, the lower was the crop performance. Among all Pheno-Phases, the *StablePhase* (i.e., the period between SD and DD) showed the highest positive correlations with harvest characteristics (except with TKW; *Pearson's r* > 0.60), demonstrating that the longer the *StablePhase*, the higher the harvest characteristics. However, *GreenUpPhase*, *Brown-DownPhase*, and *LOS* showed no or only weak correlations to harvest characteristics, suggesting that especially the start (SD) of the *StablePhase* was highly relevant for crop performance, also because SD but not DD was responsible for differences in the length of the *StablePhase*. Regarding the two PhenoSlopes, the *BrownDownSlope* was strongly positively correlated with all harvest characteristics (*Pearson's r* > 0.70; except TKW), while on the contrary, the *GreenUpSlope* had no correlations to harvest characteristics (Fig. 4). In the case of TWK, significant positive correlations were found with SD, EOS, and *BrownDownPhase*, but a negative correlation with *BrownDownSlope*, indicating that TKW was rather determined at the end of the growing season (Fig. 4).

Using those phenological metrics which significantly correlated with harvest characteristics of winter wheat (*P* < 0.05, Fig. 4), we explored the best fitting model to predict harvest characteristics (Table 3). *BrownDownPhase* and *BrownDownSlope* together explained 50.5% of the variability in TKW. For grain yield and straw yield, two and three phenological metrics explained together approximately 80% of the variability, respectively. For total N uptake and ear density, four phenological metrics explained together around 90% of the variability. Specifically, both POP and *StablePhase* (with positive coefficients) as well as SOS and EOS (with negative coefficients) explained multiple harvest characteristics.

3.2.3. Phenology explaining cropping systems effects on harvest characteristics

To facilitate the variance partitioning, we restricted the multiple regressions to a combination of cropping systems and a maximum of three phenological metrics, namely those showing the strongest relationships with all harvest characteristics (see section 2.7 for details).

SD and EOS explained 29% and 12% of the variability in grain yield, respectively (Fig. 5a). Another 26% of the variability in grain yield was explained jointly by the cropping systems, SD and EOS, and 20% together by the cropping system and SD. For straw yield, the largest fractions of the variability (24% and 23%) were explained by the combination of cropping system, SD, POP, and EOS, as well as the combination of SD and POP, respectively (Fig. 5b). In the case of total N uptake, 26% of the variability was explained by the shared fraction of EOS with cropping system, and another 20% of the variability was explained by the combination of cropping system, SOS and *StablePhase* (Fig. 5c). Similar to the results shown in Table 3, also accounting for cropping system in the variance partitioning for TKW yielded a large
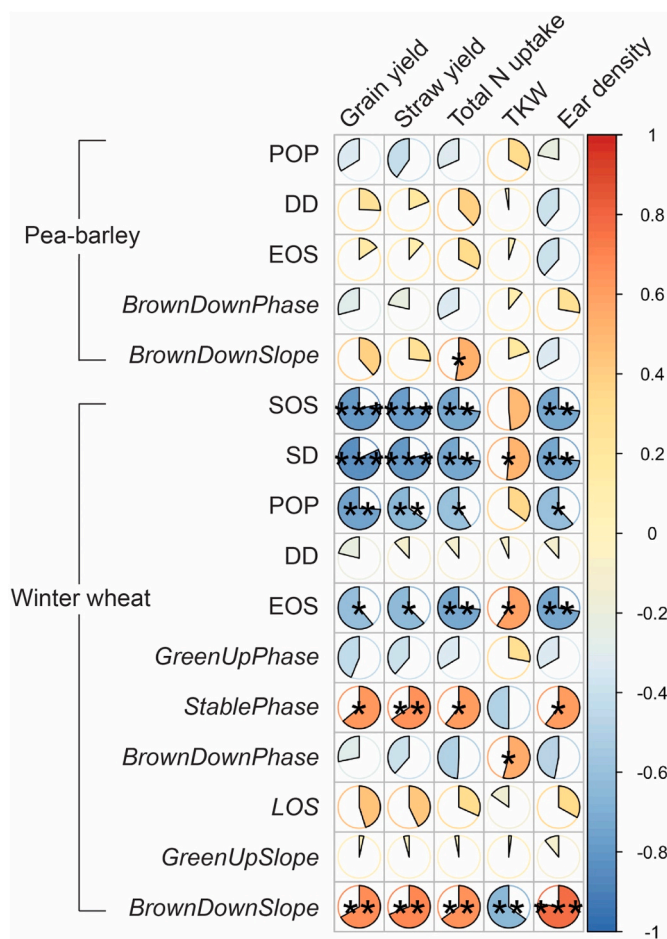

Fig. 4. Pearson correlation coefficients (*Pearson's r*) of phenological metrics and harvest characteristics, including grain yield, straw yield, total N uptake, Thousand Kernel Weight (TKW), and ear density in the pea-barley mixture (n = 15) and in winter wheat (n = 15). *Pearson's r* is given as a pie chart and is color coded. Abbreviations and explanations for all phenological metrics (PhenoTimePoints, PhenoPhases and PhenoSlopes) are given in Table 1. Levels of significance are given as * (*P* < 0.05), ** (*P* < 0.01) and *** (*P* < 0.001).

Table 3

Best fitting models explaining harvest characteristics by multiple phenological metrics for winter wheat in the year 2019. Harvest characteristics are grain yield, straw yield, total N uptake, thousand-kernel weight (TKW) and ear density. The best regression models were identified by a stepwise reduction of predictors according to the minimum AIC of the respective model.

Harvest characteristics	Model and predictors	AIC	Adjusted R^2 (%)
Grain yield (t/ha)	39.56–0.11*SD – 0.14*EOS	−19.57	80.9
Straw yield (t/ha)	48.36 + 0.12*POP – 0.20*SD – 0.22*EOS	−8.65	78.9
Total N uptake (kg N /ha)	2043.51–5.12*SOS + 3.86*POP +3.508*StablePhase – 12.44*EOS	93.72	89.7
TKW (g/1000 grain)	34.91 + 0.22*BrownDownPhase – 0.11*BrownDownSlope	15.05	50.5
Ear density(ears/m²)	1316.43–4.16*SOS + 3.79*POP +2.10*StablePhase + 1.31*BrownDownSlope	88.18	88.9

proportion of unexplained variance (residuals = 0.54). The variability in TKW was explained by *BrownDownSlope* (8%), the combination of cropping systems with *BrownDownSlope* (19%), *BrownDownPhase* (17%), and the combination of all the three factors (12%) (Fig. 5d). The biggest
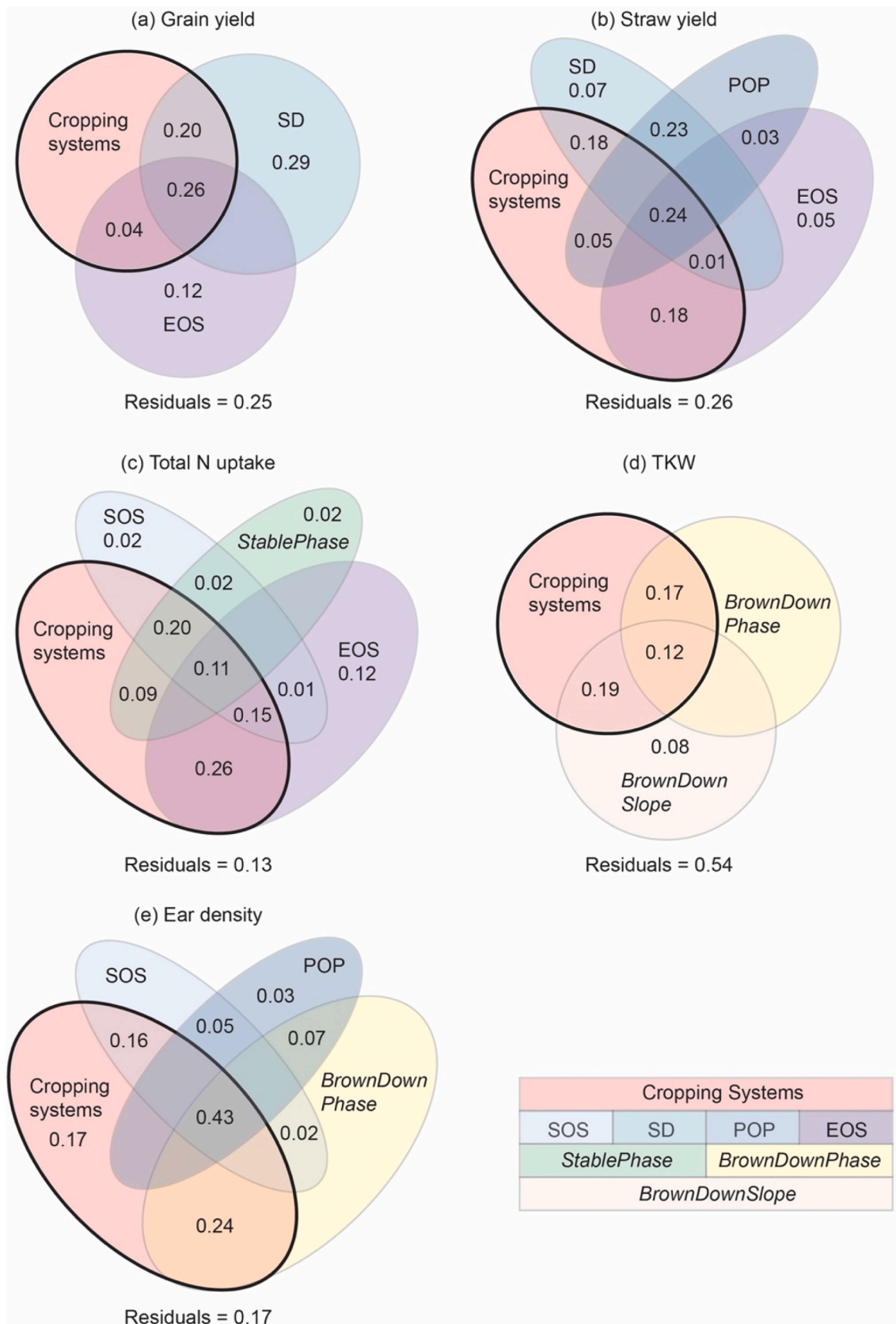
Fig. 5. Variance partitioning of the effects of cropping systems vs. phenological metrics on harvest characteristics of winter wheat: (a) grain yield, (b) straw yield, (c) total N uptake, (d) thousand kernel weight (TKW), and (e) ear density (n = 15 each). Abbreviations and explanations for all phenological metrics (PhenoTimePoints, PhenoPhases and PhenoSlopes) are given in Table 1. Numbers represent respective fractions of total variance (based on adjusted R^2). The fraction explained by cropping systems is displayed with a bold line. For further details on the variance partitioning, see methods section.

fraction of the variability in ear density (43%; Fig. 5e) was explained by the shared fraction of cropping system and SOS, POP and *BrownDownPhase*, followed by 24% of the variability in ear density explained by the shared fraction of cropping system with *BrownDownPhase*. Therefore, cropping systems by themselves did not explain any additional variability in most of the harvest characteristics (Fig. 5), except for ear density (17% explained by cropping systems).

4. Discussion

4.1. PhenoCams as an effective tool for monitoring phenology and vegetation development in arable crops

In this study, we successfully tracked the phenology of two different arable crops, a pea-barley mixture and winter wheat, based on GCC values extracted from PhenoCam images and GCC-derived phenological metrics. PhenoCam-based phenological metrics were previously used in natural and semi-natural vegetation (Klosterman et al., 2014; Richardson et al., 2018a), and only few studies were able to identify phenological metrics in annual vegetation such as summer-dry grasslands (Julitta et al., 2014; Migliavacca et al., 2011) or arable land (Aasen et al., 2020). With PhenoCams, we were able to automatically and continuously monitor crop growth near real-time, with low-cost cameras, albeit complex data processing and statistical analyses. Thus, PhenoCams monitored the peak and the growth rate of greenness, which are not detectable by a human observer. However, the complex data processing and statistical analyses might restrict the applicability of such a technique to more scientific applications unless image processing and data analyses are embedded in easy-to-use decision support tools for farmers, e.g., comparing current crop development to benchmark curves from earlier seasons. However, since smart farming and precision farming have progressed quite far and fast in recent years (Finger et al., 2019; Walter et al., 2017), the use of near-real time phenological data in early-detection or warning tools against detrimental environmental and biological impacts can be expected to be the next logical step to further develop sustainable arable agriculture, and to assess the effects of climate change on crop productivity. The application of PhenoCams can also effectively contribute to expanding agro-phenological databases with real-time observations and thus improve crop model stimulations (Ceglar et al., 2019).

To cover larger spatial scales, many studies on crop phenology are based on remote sensing data. For example, Sadeh et al. (2019) and Sakuma and Yamano (2020) used satellite observations to estimate crop growth patterns of different crops under agricultural management, suggesting the potential of high temporal resolution time series satellite imagery for crop phenology studies. Also, commercial products based on satellite imagery provide real-time field maps and help to monitor plant growth and health conditions. However, spatial and temporal resolutions usually limit the use of satellite-based data, especially in heterogeneous, fragmented ecosystems (Bégué et al., 2018; Weiss et al., 2020). In contrast, digital repeat photography with PhenoCams provides a high temporal frequency and finer spatial scale (Richardson et al., 2009), which is well suitable to track local scale crop phenology, unpick the causes of yield gaps (Duncan et al., 2015), and validate remote-sensing products (Browning et al., 2017; Richardson et al., 2018b; Thapa et al., 2021). Moreover, studies comparing PhenoCam and satellite-derived phenology found higher accuracy of PhenoCam observations in assessing the gradual process towards ripening and senescence phases (Liu et al., 2017; Yan et al., 2019). Thus, in combination with our results, we can conclude PhenoCams are highly valuable tools to continuously observe crop development.

Previous studies compared the seasonal dynamics of GCC with leaf physiological characteristics such as chlorophyll content or stand gross photosynthesis, but often only in forests (Liu et al., 2015). However, although GCC and NDVI were generally positively correlated in our study, PhenoCam phenology provided different information than field measurements of stand characteristics such as LAI, as we found a temporal mismatch between peak GCC (POP) and plant height or canopy LAI. In addition, NDVI lagged behind GCC, which is consistent with findings in forest and grassland, suggesting that GCC is more sensitive to changes in leaf color, while NDVI is sensitive to changes in leaf area and therefore stand structure (Filippa et al., 2018; Keenan et al., 2014). Thus, our results indicate that canopy greenness was rather decoupled from stand biomass production, which is usually closely related to LAI. Depending on the specific objectives of a study, a combination of different methods might therefore be needed to best assess crop performance and growth beyond phenological development.

4.2. Crop management as a driver of phenology and harvest characteristics

Although we used the same cultivar and the same sowing dates for respective crops in all cropping systems, the temporal development of the crops differed between management. However, these effects seem to be crop-specific and/or depended on the intensity of crop management, most likely driven by fertilizer additions. In total, we had five phenological metrics in common for pea-barley and winter wheat. For the unfertilized pea-barley, we found only one out of five phenological metrics being significantly affected by cropping systems, while there were three out of five phenological metrics for the fertilized winter wheat. Effects of crop management on phenology are in line with previous studies, which reported crop phenology to respond to different fertilization intensities (meta-analysis by Wang and Tang, 2019) and different levels of tillage (Basir et al., 2016; Chevalier and Ciha, 1986; Engel et al., 2009).

We demonstrated that early-stage PhenoTimePoints (only recorded in winter wheat) and peak greenness (recorded in both crops) were more affected by cropping systems than the late-stage PhenoTimePoints. This suggests that management practices, which change the conditions during the early growing season, might impact crop yield most. Late phenological stages might depend more on weather and seasonal changes and are thus less responsive to crop management. In this respect, organic farming is known to affect plant health, soil fertility and N losses (Röös et al., 2018). In spring, the availability of mineral N in soil is usually lower with only organic fertilizers than with mineral fertilizer (Barlóg et al., 2020; Dahlin et al., 2005). Thus, the delay in phenology in organic farming might be due to low nitrogen availability, limiting the early establishment and growth of crops, which, as reported in other studies (e.g., Olesen et al., 2007, led to organic crops not being able to efficiently suppress weed development). Weeds were also observed in our images and thus considered together with crops in the calculations of GCC and phenology metrics. However, weed biomass accounted for only a small proportion of the total biomass at harvest (5.3% of pea-barley mixture, 2.7% of winter wheat). Therefore, the potential bias created by weeds was negligible.

We observed an initial growth lag under no/reduced tillage systems. Thus, the negative effects of conservation tillage such as increased prevalence of pests or weeds (Fernández-Ugalde et al., 2009; Mohler, 1993), lower quality of seed placement (Van den Putte et al., 2010), greater penetration resistance (Fernández-Ugalde et al., 2009; Lamp-urlanés and Cantero-Martínez, 2003) and delayed soil warming (Rasmussen, 1999) seemed to have outweighed possible benefits such as increased water availability (Holland, 2004) or greater water storge (Su et al., 2007) in our study. A lower mineralization rate in no/reduced tillage compared to conventional tillage (Six et al., 2002) is also likely to be detrimental for initial crop growth. Additionally, significantly lower root biomass could be observed under no/reduced compared to conventional tillage (Haddaway et al., 2017), suggesting that root growth might have been hampered, resulting in the initial growth lag under no/reduced tillage in our study.

Grain yield differed between organic and conventional systems only for winter wheat, most likely because nitrogen supply was lower with

organic fertilizer compared to mineral fertilizer (Askegaard et al., 2011). However, this difference was not observed in the pea-barley mixture, where no fertilizer was applied. Since legumes have been reported to have a considerably smaller yield gap than cereals when either one is grown in monoculture (Röös et al., 2018), growing a mixture of legumes (pea) with cereals (barley) was obviously beneficial to overcome this yield gap. This clearly illustrates the potential of legumes to increase yield in low-input arable agriculture by intercropping.

4.3. Crop phenology as a driver for harvest characteristics

Many previous studies have pointed out the importance of growing season length for harvest characteristics (Mueller et al., 2015), e.g., using growing season length to predict crop yield (Gadanakis and Areal, 2020; Jägermeyr and Frieler, 2018). However, in our study, we demonstrated for the first time that the timing of the start of high GCC values (SD) was more important than the length of the period with high GCC values (*StablePhase*), as SD explained more variations in grain and straw yield than the *StablePhase* (Fig. 5). Noticeably, early-stage phenological metrics such as SD and POP contributed to the large fraction of explained variation in grain yield (29% only explained by SD) and straw yield (7% only by SD; 23% shared by SD and POP), much larger than the fraction of variability explained only by the late-stage EOS (12% for grain yield; 5% for straw yield). This is in agreement with de Cárcer et al. (2019) who showed that climatic conditions around the heading phase, thus during the early crop development, explained about 22% of the variance in long-term wheat yields, while the effects of soil tillage and late-stage phenological metrics on yield were negligible. In contrast to yield, EOS explained a larger share of the variability in total N uptake (12% only by EOS) than early-stage phenological metrics in our study (2% only by SOS; Fig. 5). TKW was also rather determined by late-stage phenological metrics, i.e., *BrownDownPhase* and *BrownDownSlope*, which is not surprising as grain formation and filling happened exactly during this late phase. Overall, our results suggest that the timing of early crop establishment is crucial for the final yield, while the timing towards the end of growing season is relevant for TKW.

Moreover, the tight links between vegetation indices and yield support earlier studies using NDVI, either derived from remote sensing data (Shammi and Meng, 2021) or drone-mounted hyperspectral cameras (Herrmann et al., 2020). Fernandez-Gallego and colleagues highlighted that the differences in canopy color were key in assessing grain yield of wheat (Fernandez-Gallego et al., 2019). The use of RGB imagery was reported to be highly relevant in estimating barley biomass (Brocks and Bareth, 2018).

4.4. Phenology explains the effects of cropping systems on harvest characteristics

Disentangling the combined effects of cropping system and phenology on harvest characteristics, our study has shown that cropping systems did not explain any additional share of the variability in any of the harvest characteristics when phenology was included in the models. This can be seen as an indication that cropping system effects on harvest characteristics act strongly via changes in crop phenology. Other effects of cropping systems, such as differences in fertilizer dosing and timing, nutrient availability, and the competition of crops and weeds (Birkhofer et al., 2008; Wittwer et al., 2017) were integrated in these phenological shifts, and cannot be assessed separately in our study system. Otherwise, cropping systems would have explained an individual share of the variability in harvest characteristics, in addition to what was explained by phenology. Up to now, lower yields in organic farming has been explained by lower available fertilizer, higher pest damage, and weed pressure in comparison to conventional farming (Röös et al., 2018). In this study, we demonstrated that delayed phenology acted as an important factor that caused lower yield in organic farming compared to conventional farming.

Phenological metrics were strongly correlated with harvest characteristics only for winter wheat but not for pea-barley. One of the reasons might be that–other than for winter wheat–most of the harvest characteristics for pea-barley mixture were unaffected by cropping systems, most likely because crop management in the unfertilized and unsprayed pea-barley mixture was generally less intensive and thus resulted in smaller differences among the four cropping systems compared to winter wheat. This indicates that the relationship between phenology and crop yield might only become evident once cropping systems considerably affect crop phenology and especially crop yield.

5. Conclusions

Our results clearly demonstrated the possibility of tracking crop phenology and growth dynamics with PhenoCams, representing a valuable tool for high-resolution temporal monitoring of crops in science, and potentially also in practice. We found strong effects of crop management on crop phenology, in particular delayed phenology by organic and reduced/no-tillage practices, resulting in lower crop yields for winter wheat. This finding adds a new, highly relevant aspect to the discussion about the mechanisms of potential yield-gaps in organic and conservation agriculture. However, future research needs to test if cropping system effects on harvest characteristics acting via changes in crop phenology also occur for other crops than the ones studied here. Moreover, if these findings also hold true under conditions with environmental stress, e.g., during a drought, remains to be investigated. This will help to understand the effects of crop management and environmental drivers such as climate change on food production, the selection of suitable crop varieties, and the temporal adjustment of management practices to optimize cropping systems.

Declaration of Competing Interest

The authors declare that they have no known competing financial interests or personal relationships that could have appeared to influence the work reported in this paper.

Appendix A. Supplementary data

Supplementary data to this article can be found online at https://doi.org/10.1016/j.agsy.2021.103306.

References

Aasen, H., Kirchgessner, N., Walter, A., Liebisch, F., 2020. PhenoCams for Field Phenotyping: using very high temporal resolution digital repeated photography to investigate interactions of growth, phenology, and harvest traits. Front. Plant Sci. 11, 593. https://doi.org/10.3389/fpls.2020.00593.

Ahrends, H., Etzold, S., Kutsch, W., Stoeckli, R., Bruegger, R., Jeanneret, F., Wanner, H., Buchmann, N., Eugster, W., 2009. Tree phenology and carbon dioxide fluxes: use of digital photography for process-based interpretation at the ecosystem scale. Clim. Res. 39, 261–274. https://doi.org/10.3354/cr00811.

Askegaard, M., Olesen, J.E., Rasmussen, I.A., Kristensen, K., 2011. Nitrate leaching from organic arable crop rotations is mostly determined by autumn field management. Agric. Ecosyst. Environ. 142, 149–160. https://doi.org/10.1016/j.agee.2011.04.014.

Baldocchi, D., 2008. 'Breathing' of the terrestrial biosphere: lessons learned from a global network of carbon dioxide flux measurement systems. Aust. J. Bot. https://doi.org/10.1071/BT07151.

Barłóg, P., Hlisnikovský, L., Kunzová, E., 2020. Effect of digestate on soil organic carbon and plant-available nutrient content compared to cattle slurry and mineral fertilization. Agronomy 10, 379. https://doi.org/10.3390/agronomy10030379.

Basir, A., Jan, M.T., Arif, M., Khan, M.J., 2016. Response of tillage, nitrogen and stubble management on phenology and crop establishment of wheat. Int. J. Agric. Biol. 18, 1–8. https://doi.org/10.17957/IJAB/14.0030.

Bates, D., Mächler, M., Bolker, B.M., Walker, S.C., 2015. Fitting linear mixed-effects models using lme4. J. Stat. Softw. 67 https://doi.org/10.18637/jss.v067.i01.

Beck, P.S.A., Atzberger, C., Høgda, K.A., Johansen, B., Skidmore, A.K., 2006. Improved monitoring of vegetation dynamics at very high latitudes: A new method using MODIS NDVI. Remote Sens. Environ. 100, 321–334. https://doi.org/10.1016/j.rse.2005.10.021.

Bégué, A., Arvor, D., Bellon, B., Betbeder, J., de Abelleyra, D., Ferraz, R.P.D., Lebourgeois, V., Lelong, C., Simões, M., Verón, S.R., 2018. Remote sensing and cropping practices: A review. Remote Sens. https://doi.org/10.3390/rs10010099.

Birkhofer, K., Bezemer, T.M., Bloem, J., Bonkowski, M., Christensen, S., Dubois, D., Ekelund, F., Fließbach, A., Gunst, L., Hedlund, K., Mäder, P., Mikola, J., Robin, C., Setälä, H., Tatin-Froux, F., Van der Putten, W.H., Scheu, S., 2008. Long-term organic farming fosters below and aboveground biota: Implications for soil quality, biological control and productivity. Soil Biol. Biochem. 40, 2297–2308. https://doi.org/10.1016/j.soilbio.2008.05.007.

Brocks, S., Bareth, G., 2018. Estimating barley biomass with crop surface models from oblique RGB imagery. Remote Sens. 10, 268. https://doi.org/10.3390/rs10020268.

Brown, T.B., Hultine, K.R., Steltzer, H., Denny, E.G., Denslow, M.W., Granados, J., Henderson, S., Moore, D., Nagai, S., SanClements, M., Sánchez-Azofeifa, A., Sonnentag, O., Tazik, D., Richardson, A.D., 2016. Using phenocams to monitor our changing Earth: toward a global phenocam network. Front. Ecol. Environ. 14, 84–93. https://doi.org/10.1002/fee.1222.

Browning, D.M., Karl, J.W., Morin, D., Richardson, A.D., Tweedie, C.E., 2017. Phenocams bridge the gap between field and satellite observations in an arid grassland ecosystem. Remote Sens. 9, 1071. https://doi.org/10.3390/rs9101071.

Ceglar, A., van der Wijngaart, R., de Wit, A., Lecerf, R., Boogaard, H., Seguini, L., van den Berg, M., Toreti, A., Zampieri, M., Fumagalli, D., Baruth, B., 2019. Improving WOFOST model to simulate winter wheat phenology in Europe: Evaluation and effects on yield. Agric. Syst. 168, 168–180. https://doi.org/10.1016/j.agsy.2018.05.002.

Chen, S., Huang, Y., Gao, S., Wang, G., 2019. Impact of physiological and phenological change on carbon uptake on the Tibetan Plateau revealed through GPP estimation based on spaceborne solar-induced fluorescence. Sci. Total Environ. 663, 45–59. https://doi.org/10.1016/j.scitotenv.2019.01.324.

Chevalier, P.M., Ciha, A.J., 1986. Influence of tillage on phenology and carbohydrate metabolism of spring wheat. Agron. J. 78, 296–300. https://doi.org/10.2134/agronj1986.00021962007800020017x.

Churkina, G., Schimel, D., Braswell, B.H., Xiao, X., 2005. Spatial analysis of growing season length control over net ecosystem exchange. Glob. Chang. Biol. 11, 1777–1787. https://doi.org/10.1111/j.1365-2486.2005.001012.x.

Craufurd, P.Q., Wheeler, T.R., 2009. Climate change and the flowering time of annual crops. J. Exp. Bot. 60, 2529–2539. https://doi.org/10.1093/jxb/erp196.

Dahlin, S., Kirchmann, H., Kätterer, T., Gunnarsson, S., Bergström, L., 2005. Possibilities for improving nitrogen use from organic materials in agricultural cropping systems. In: Ambio. Kluwer Academic Publishers, pp. 288–295. https://doi.org/10.1579/0044-7447-34.4.288.

de Cárcer, P.S., Sinaj, S., Santonja, M., Fossati, D., Jeangros, B., 2019. Long-term effects of crop succession, soil tillage and climate on wheat yield and soil properties. Soil Tillage Res. 190, 209–219. https://doi.org/10.1016/j.still.2019.01.012.

de Castro, A.I., Six, J., Plant, R.E., Peña, J.M., 2018. Mapping crop calendar events and phenology-related metrics at the parcel level by object-based image analysis (OBIA) of MODIS-NDVI time-series: A case study in central California. Remote Sens. 10, 1745. https://doi.org/10.3390/rs10111745.

Du, Q., Liu, H.Z., Li, Y., Xu, L., Diloksumpun, S., 2019. The effect of phenology on the carbon exchange process in grassland and maize cropland ecosystems across a semiarid area of China. Sci. Total Environ. 695 (133), 868. https://doi.org/10.1016/j.scitotenv.2019.133868.

Duncan, J.M.A., Dash, J., Atkinson, P.M., 2015. The potential of satellite-observed crop phenology to enhance yield gap assessments in smallholder landscapes. Front. Environ. Sci. https://doi.org/10.3389/fenvs.2015.00056.

Engel, F.L., Bertol, I., Ritter, S.R., Paz González, A., Paz-Ferreiro, J., Vidal Vázquez, E., 2009. Soil erosion under simulated rainfall in relation to phenological stages of soybeans and tillage methods in Lages, SC. Brazil. Soil Tillage Res. 103, 216–221. https://doi.org/10.1016/j.still.2008.05.017.

Estrada-Medina, H., Santiago, L.S., Graham, R.C., Allen, M.F., Jiménez-Osornio, J.J., 2013. Source water, phenology and growth of two tropical dry forest tree species growing on shallow karst soils. Trees - Struct. Funct. 27, 1297–1307. https://doi.org/10.1007/s00468-013-0878-9.

Eyshi Rezaei, E., Siebert, S., Ewert, F., 2017. Climate and management interaction cause diverse crop phenology trends. Agric. For. Meteorol. 233, 55–70. https://doi.org/10.1016/j.agrformet.2016.11.003.

Fernandez-Gallego, J.A., Kefauver, S.C., Vatter, T., Aparicio Gutiérrez, N., Nieto-Taladriz, M.T., Araus, J.L., 2019. Low-cost assessment of grain yield in durum wheat using RGB images. Eur. J. Agron. 105, 146–156. https://doi.org/10.1016/j.eja.2019.02.007.

Fernández-Ugalde, O., Virto, I., Bescansa, P., Imaz, M.J., Enrique, A., Karlen, D.L., 2009. No-tillage improvement of soil physical quality in calcareous, degradation-prone, semiarid soils. Soil Tillage Res. 106, 29–35. https://doi.org/10.1016/j.still.2009.09.012.

Filippa, G., Cremonese, E., Migliavacca, M., Galvagno, M., Forkel, M., Wingate, L., Tomelleri, E., Morra di Cella, U., Richardson, A.D., 2016. Phenopix: A R package for image-based vegetation phenology. Agric. For. Meteorol. 220, 141–150. https://doi.org/10.1016/J.AGRFORMET.2016.01.006.

Filippa, G., Cremonese, E., Migliavacca, M., Galvagno, M., Sonnentag, O., Humphreys, E., Hufkens, K., Ryu, Y., Verfaillie, J., Morra di Cella, U., Richardson, A.D., 2018. NDVI derived from near-infrared-enabled digital cameras: Applicability across different plant functional types. Agric. For. Meteorol. 249, 275–285. https://doi.org/10.1016/j.agrformet.2017.11.003.

Finger, R., Swinton, S.M., El Benni, N., Walter, A., 2019. Precision farming at the nexus of agricultural production and the environment. Annu. Rev. Resour. Econ. https://doi.org/10.1146/annurev-resource-100,518-093929.

Gadanakis, Y., Areal, F.J., 2020. Accounting for rainfall and the length of growing season in technical efficiency analysis. Oper. Res. 20, 2583–2608. https://doi.org/10.1007/s12351-018-0429-7.

Gao, F., Zhang, X., 2021. Mapping crop phenology in near real-time using satellite remote sensing: challenges and opportunities. J. Remote Sens. 2021, 1–14. https://doi.org/10.34133/2021/8379391.

Garrity, S.R., Bohrer, G., Maurer, K.D., Mueller, K.L., Vogel, C.S., Curtis, P.S., 2011. A comparison of multiple phenology data sources for estimating seasonal transitions in deciduous forest carbon exchange. Agric. For. Meteorol. 151, 1741–1752. https://doi.org/10.1016/j.agrformet.2011.07.008.

Gattinger, A., Muller, A., Haeni, M., Skinner, C., Fliessbach, A., Buchmann, N., Mäder, P., Stolze, M., Smith, P., Scialabba, N.E.H., Niggli, U., 2012. Enhanced top soil carbon stocks under organic farming. Proc. Natl. Acad. Sci. U. S. A. 109, 18,226–18,231. https://doi.org/10.1073/pnas.1209429109.

Gu, L., Post, W.M., Baldocchi, D.D., Black, T.A., Suyker, A.E., Verma, S.B., Vesala, T., Wofsy, S.C., 2009. Characterizing the seasonal dynamics of plant community photosynthesis across a range of vegetation types. In: Phenology of Ecosystem Processes: Applications in Global Change Research. Springer, New York, New York, NY, pp. 35–58. https://doi.org/10.1007/978-1-4419-0026-5_2.

Haddaway, N.R., Hedlund, K., Jackson, L.E., Kätterer, T., Lugato, E., Thomsen, I.K., Jørgensen, H.B., Isberg, P.E., 2017. How does tillage intensity affect soil organic carbon? A systematic review. Environ. Evid. https://doi.org/10.1186/s13750-017-0108-9.

Herrmann, I., Bdolach, E., Montekyo, Y., Rachmilevitch, S., Townsend, P.A., Karnieli, A., 2020. Assessment of maize yield and phenology by drone-mounted superspectral camera. Precis. Agric. 21, 51–76. https://doi.org/10.1007/s11119-019-09659-5.

Hoffmann, M., Pohl, M., Jurisch, N., Prescher, A.K., Mendez Campa, E., Hagemann, U., Remus, R., Verch, G., Sommer, M., Augustin, J., 2018. Maize carbon dynamics are driven by soil erosion state and plant phenology rather than nitrogen fertilization form. Soil Tillage Res. 175, 255–266. https://doi.org/10.1016/j.still.2017.09.004.

Holland, J.M., 2004. The environmental consequences of adopting conservation tillage in Europe: Reviewing the evidence. Agric. Ecosyst. Environ. https://doi.org/10.1016/j.agee.2003.12.018.

Huang, Y., Ren, W., Wang, L., Hui, D., Grove, J.H., Yang, X., Tao, B., Goff, B., 2018. Greenhouse gas emissions and crop yield in no-tillage systems: A meta-analysis. Agric. Ecosyst. Environ. 268, 144–153. https://doi.org/10.1016/j.agee.2018.09.002.

Hufkens, K., Friedl, M., Sonnentag, O., Braswell, B.H., Milliman, T., Richardson, A.D., 2012. Linking near-surface and satellite remote sensing measurements of deciduous broadleaf forest phenology. Remote Sens. Environ. 117, 307–321. https://doi.org/10.1016/j.rse.2011.10.006.

Jägermeyr, J., Frieler, K., 2018. Spatial variations in crop growing seasons pivotal to reproduce global fluctuations in maize and wheat yields. Sci. Adv. 4, eaat4517. https://doi.org/10.1126/sciadv.aat4517.

Julitta, T., Cremonese, E., Migliavacca, M., Colombo, R., Galvagno, M., Siniscalco, C., Rossini, M., Fava, F., Cogliati, S., Morra di Cella, U., Menzel, A., 2014. Using digital camera images to analyse snowmelt and phenology of a subalpine grassland. Agric. For. Meteorol. 198–199, 116–125. https://doi.org/10.1016/j.agrformet.2014.08.007.

Keenan, T.F., Darby, B., Felts, E., Sonnentag, O., Friedl, M.A., Hufkens, K., O'Keefe, J., Klosterman, S., Munger, J.W., Toomey, M., Richardson, A.D., 2014. Tracking forest phenology and seasonal physiology using digital repeat photography: A critical assessment. Ecol. Appl. 24, 1478–1489. https://doi.org/10.1890/13-0652.1.

Klepeckas, M., Januškaitienė, I., Vagusevičienė, I., Juknys, R., 2020. Effects of different sowing time to phenology and yield of winter wheat. Agric. Food Sci. 29, 346–358. https://doi.org/10.23986/afsci.90013.

Klosterman, S.T., Hufkens, K., Gray, J.M., Melaas, E., Sonnentag, O., Lavine, I., Mitchell, L., Norman, R., Friedl, M.A., Richardson, A.D., 2014. Evaluating remote sensing of deciduous forest phenology at multiple spatial scales using PhenoCam imagery. Biogeosciences 11, 4305–4320. https://doi.org/10.5194/bg-11-4305-2014.

Knapp, S., van der Heijden, M.G.A., 2018. A global meta-analysis of yield stability in organic and conservation agriculture. Nat. Commun. 9 https://doi.org/10.1038/s41467-018-05956-1.

Lampurlanés, J., Cantero-Martínez, C., 2003. Soil bulk density and penetration resistance under different tillage and crop management systems and their relationship with barley root growth. Agron. J. 95, 526–536. https://doi.org/10.2134/agronj2003.5260.

Liu, Z., Hu, H., Yu, H., Yang, X., Yang, H., Ruan, C., Wang, Y., Tang, J., 2015. Relationship between leaf physiologic traits and canopy color indices during the leaf expansion period in an oak forest. Ecosphere 6, art259. https://doi.org/10.1890/ES14-00452.1.

Liu, J., Huffman, T., Shang, J., Qian, B., Dong, T., Zhang, Y., Jing, Q., 2016. Estimation of crop yield in regions with mixed crops using different cropland masks and time-

series MODIS data. In: International Geoscience and Remote Sensing Symposium (IGARSS). Institute of Electrical and Electronics Engineers Inc, pp. 7161–7163. https://doi.org/10.1109/IGARSS.2016.7730868.

Liu, Y., Hill, M.J., Zhang, X., Wang, Z., Richardson, A.D., Hufkens, K., Filippa, G., Baldocchi, D.D., Ma, S., Verfaillie, J., Schaaf, C.B., 2017. Using data from Landsat, MODIS, VIIRS and PhenoCams to monitor the phenology of California oak/grass savanna and open grassland across spatial scales. Agric. For. Meteorol. 237–238, 311–325. https://doi.org/10.1016/j.agrformet.2017.02.026.

Loaiza Puerta, V., Pujol Pereira, E.I., Wittwer, R., van der Heijden, M., Six, J., 2018. Improvement of soil structure through organic crop management, conservation tillage and grass-clover ley. Soil Tillage Res. 180, 1–9. https://doi.org/10.1016/j.still.2018.02.007.

Lumley, T., 2020. R Package "leaps" , Regression Subset Selection [WWW Document]. R J. URL. https://cran.r-project.org/package=leaps.

Macgregor, C.J., Thomas, C.D., Roy, D.B., Beaumont, M.A., Bell, J.R., Brereton, T., Bridle, J.R., Dytham, C., Fox, R., Gotthard, K., Hoffmann, A.A., Martin, G., Middlebrook, I., Nylin, S., Platts, P.J., Rasteiro, R., Saccheri, I.J., Villoutreix, R., Wheat, C.W., Hill, J.K., 2019. Climate-induced phenology shifts linked to range expansions in species with multiple reproductive cycles per year. Nat. Commun. 10, 1–10. https://doi.org/10.1038/s41467-019-12,479-w.

MeteoSwiss, 2020. Federal office of meteorology and climatology MeteoSwiss, URL. https://www.meteoswiss.admin.ch/home.html?tab=overview.

Migliavacca, M., Galvagno, M., Cremonese, E., Rossini, M., Meroni, M., Sonnentag, O., Cogliati, S., Manca, G., Diotri, F., Busetto, L., Cescatti, A., Colombo, R., Fava, F., Morra di Cella, U., Pari, E., Siniscalco, C., Richardson, A.D., 2011. Using digital repeat photography and eddy covariance data to model grassland phenology and photosynthetic CO_2 uptake. Agric. For. Meteorol. 151, 1325–1337. https://doi.org/10.1016/j.agrformet.2011.05.012.

Mo, F., Sun, M., Liu, X.Y., Wang, J.Y., Zhang, X.C., Ma, B.L., Xiong, Y.C., 2016. Phenological responses of spring wheat and maize to changes in crop management and rising temperatures from 1992 to 2013 across the Loess Plateau. F. Crop. Res. 196, 337–347. https://doi.org/10.1016/j.fcr.2016.06.024.

Mohler, C.L., 1993. A model of the effects of tillage on emergence of weed seedlings. Ecol. Appl. 3, 53–73. https://doi.org/10.2307/1941792.

Mueller, B., Hauser, M., Iles, C., Rimi, R.H., Zwiers, F.W., Wan, H., 2015. Lengthening of the growing season in wheat and maize producing regions. Weather Clim. Extrem. 9, 47–56. https://doi.org/10.1016/j.wace.2015.04.001.

Nord, E.A., Lynch, J.P., 2009. Plant phenology: A critical controller of soil resource acquisition. J. Exp. Bot. https://doi.org/10.1093/jxb/erp018.

Oksanen, J., Blanchet, F.G., Friendly, M., Kindt, R., Legendre, P., Mcglinn, D., Minchin, P. R., O'hara, R.B., Simpson, G.L., Solymos, P., Henry, M., Stevens, H., Szoecs, E., Maintainer, H.W., 2020. Package "vegan" Title Community Ecology Package Version 2, pp. 5–7.

Olesen, J.E., Hansen, E.M., Askegaard, M., Rasmussen, I.A., 2007. The value of catch crops and organic manures for spring barley in organic arable farming. F. Crop. Res. 100, 168–178. https://doi.org/10.1016/j.fcr.2006.07.001.

Papale, D., Reichstein, M., Aubinet, M., Canfora, E., Bernhofer, C., Kutsch, W., Longdoz, B., Rambal, S., Valentini, R., Vesala, T., Yakir, D., 2006. Towards a standardized processing of Net Ecosystem Exchange measured with eddy covariance technique: algorithms and uncertainty estimation. Biogeosciences 3, 571–583. https://doi.org/10.5194/bg-3-571-2006.

Piao, S., Liu, Q., Chen, A., Janssens, I.A., Fu, Y., Dai, J., Liu, L., Lian, X., Shen, M., Zhu, X., 2019. Plant phenology and global climate change: Current progresses and challenges. Glob. Chang. Biol. https://doi.org/10.1111/gcb.14619.

Pittelkow, C.M., Linquist, B.A., Lundy, M.E., Liang, X., van Groenigen, K.J., Lee, J., van Gestel, N., Six, J., Venterea, R.T., van Kessel, C., 2015. When does no-till yield more? A global meta-analysis. F. Crop. Res. 183, 156–168. https://doi.org/10.1016/j.fcr.2015.07.020.

R Code Team, 2020. A language and environment for statistical computing. R Foundation for Statistical Computing.

Rasmussen, K.J., 1999. Impact of ploughless soil tillage on yield and soil quality: A Scandinavian review. Soil Tillage Res. 53, 3–14. https://doi.org/10.1016/S0167-1987(99)00072-0.

Reganold, J.P., Wachter, J.M., 2016. Organic agriculture in the twenty-first century. Nat. plants. https://doi.org/10.1038/nplants.2015.221.

Rezaei, E.E., Siebert, S., Hüging, H., Ewert, F., 2018. Climate change effect on wheat phenology depends on cultivar change. Sci. Rep. 8, 1–10. https://doi.org/10.1038/s41598-018-23,101-2.

Richardson, A.D., Braswell, B.H., Hollinger, D.Y., Jenkins, J.P., Ollinger, S.V., 2009. Near-surface remote sensing of spatial and temporal variation in canopy phenology. Ecol. Appl. 19, 1417–1428. https://doi.org/10.1890/08-2022.1.

Richardson, A.D., Hufkens, K., Milliman, T., Aubrecht, D.M., Chen, M., Gray, J.M., Johnston, M.R., Keenan, T.F., Klosterman, S.T., Kosmala, M., Melaas, E.K., Friedl, M. A., Frolking, S., 2018a. Tracking vegetation phenology across diverse North American biomes using PhenoCam imagery. Sci. Data 5, 1–24. https://doi.org/10.1038/sdata.2018.28.

Richardson, A.D., Hufkens, K., Milliman, T., Frolking, S., 2018b. Intercomparison of phenological transition dates derived from the PhenoCam Dataset V1.0 and MODIS satellite remote sensing. Sci. Rep. 8, 1–12. https://doi.org/10.1038/s41598-018-23,804-6.

Richner, W., Sinaj, S., 2017. Grundlagen für die Düngung landwirtschaftlicher Kulturen in der Schweiz (GRUD 2017). Agrar, Schweiz, p. 8.

Röös, E., Mie, A., Wivstad, M., Salomon, E., Johansson, B., Gunnarsson, S., Wallenbeck, A., Hoffmann, R., Nilsson, U., Sundberg, C., Watson, C.A., 2018. Risks and opportunities of increasing yields in organic farming. A review. Agron. Sustain. Dev. https://doi.org/10.1007/s13593-018-0489-3.

Sadeh, Y., Zhu, X., Chenu, K., Dunkerley, D., 2019. Sowing date detection at the field scale using CubeSats remote sensing. Comput. Electron. Agric. 157, 568–580. https://doi.org/10.1016/j.compag.2019.01.042.

Sakuma, A., Yamano, H., 2020. Satellite constellation reveals crop growth patterns and improves mapping accuracy of cropping practices for subtropical small-scale fields in Japan. Remote Sens. 12, 2419. https://doi.org/10.3390/RS12152419.

Schoving, C., Stöckle, C.O., Colombet, C., Champolivier, L., Debaeke, P., Maury, P., 2020. Combining simple phenotyping and photothermal algorithm for the prediction of soybean phenology: application to a range of common cultivars grown in Europe. Front. Plant Sci. 10, 1755. https://doi.org/10.3389/fpls.2019.01755.

Seitz, S., Goebes, P., Puerta, V.L., Pereira, E.I.P., Wittwer, R., Six, J., van der Heijden, M. G.A., Scholten, T., 2019. Conservation tillage and organic farming reduce soil erosion. Agron. Sustain. Dev. 39, 1–10. https://doi.org/10.1007/s13593-018-0545-z.

Shammi, S.A., Meng, Q., 2021. Use time series NDVI and EVI to develop dynamic crop growth metrics for yield modeling. Ecol. Indic. 121 (107), 124. https://doi.org/10.1016/j.ecolind.2020.107124.

Six, J., Feller, C., Denef, K., Ogle, S.M., De Moraes Sa, J.C., Albrecht, A., 2002. Soil organic matter, biota and aggregation in temperate and tropical soils - Effects of no-tillage, in: Agronomie. EDP Sciences 755–775. https://doi.org/10.1051/agro:2002043.

Skinner, C., Gattinger, A., Krauss, M., Krause, H.M., Mayer, J., van der Heijden, M.G.A., Mäder, P., 2019. The impact of long-term organic farming on soil-derived greenhouse gas emissions. Sci. Rep. 9, 1–10. https://doi.org/10.1038/s41598-018-38,207-w.

Sonnentag, O., Hufkens, K., Teshera-Sterne, C., Young, A.M., Friedl, M., Braswell, B.H., Milliman, T., O'Keefe, J., Richardson, A.D., 2012. Digital repeat photography for phenological research in forest ecosystems. Agric. For. Meteorol. 152, 159–177. https://doi.org/10.1016/j.agrformet.2011.09.009.

Su, Z., Zhang, J., Wu, W., Cai, D., Lv, J., Jiang, G., Huang, J., Gao, J., Hartmann, R., Gabriels, D., 2007. Effects of conservation tillage practices on winter wheat water-use efficiency and crop yield on the Loess Plateau. China. Agric. Water Manag. 87, 307–314. https://doi.org/10.1016/j.agwat.2006.08.005.

Thapa, S., Garcia Millan, V.E., Eklundh, L., 2021. Assessing forest phenology: A multi-scale comparison of near-surface (UAV, spectral reflectance sensor, phenocam) and satellite (MODIS, sentinel-2) remote sensing. Remote Sens. 13, 1597. https://doi.org/10.3390/rs13081597.

Toomey, M., Friedl, M.A., Frolking, S., Hufkens, K., Klosterman, S., Sonnentag, O., Baldocchi, D.D., Bernacchi, C.J., Biraud, S.C., Bohrer, G., Brzostek, E., Burns, S.P., Coursolle, C., Hollinger, D.Y., Margolis, H.A., McCaughey, H., Monson, R.K., Munger, J.W., Pallardy, S., Phillips, R.P., Torn, M.S., Wharton, S., Zeri, M., Richardson, A.D., 2015. Greenness indices from digital cameras predict the timing and seasonal dynamics of canopy-scale photosynthesis. Ecol. Appl. 25, 99–115. https://doi.org/10.1890/14-0005.1.

Van den Putte, A., Govers, G., Diels, J., Gillijns, K., Demuzere, M., 2010. Assessing the effect of soil tillage on crop growth: A meta-regression analysis on European crop yields under conservation agriculture. Eur. J. Agron. 33, 231–241. https://doi.org/10.1016/j.eja.2010.05.008.

Verhulst, N., Govaerts, B., Nelissen, V., Sayre, K.D., Crossa, J., Raes, D., Deckers, J., 2011. The effect of tillage, crop rotation and residue management on maize and wheat growth and development evaluated with an optical sensor. F. Crop. Res. 120, 58–67. https://doi.org/10.1016/j.fcr.2010.08.012.

Walter, A., Finger, R., Huber, R., Buchmann, N., 2017. Smart farming is key to developing sustainable agriculture. Proc. Natl. Acad. Sci. U. S. A. https://doi.org/10.1073/pnas.1707462114.

Wang, C., Tang, Y., 2019. Responses of plant phenology to nitrogen addition: a meta-analysis. Oikos 128, 1243–1253. https://doi.org/10.1111/oik.06099.

Weiss, M., Jacob, F., Duveiller, G., 2020. Remote sensing for agricultural applications: A meta-review. Remote Sens. Environ. 236 (111), 402. https://doi.org/10.1016/j.rse.2019.111402.

Wingate, L., Ogée, J., Cremonese, E., Filippa, G., Mizunuma, T., Migliavacca, M., Moisy, C., Wilkinson, M., Moureaux, C., Wohlfahrt, G., Hammerle, A., Hörtnagl, L., Gimeno, C., Porcar-Castell, A., Galvagno, M., Nakaji, T., Morison, J., Kolle, O., Knohl, A., Kutsch, W., Kolari, P., Nikinmaa, E., Levula, J., Heinesch, B., Sprintsin, M., Yakir, D., Manise, T., Guyon, D., Ahrends, H., Plaza-Aguilar, A., Guan, J.H., Grace, J., 2015. Interpreting canopy development and physiology using a European phenology camera network at flux sites. Biogeosciences 12, 24. https://doi.org/10.5194/bg-12-5995-2015.

Wittwer, R.A., Dorn, B., Jossi, W., Van Der Heijden, M.G.A., 2017. Cover crops support ecological intensification of arable cropping systems. Sci. Rep. 7, 1–12. https://doi.org/10.1038/srep41911.

Xia, J., Niu, S., Ciais, P., Janssens, I.A., Chen, J., Ammann, C., Arain, A., Blanken, P.D., Cescatti, A., Bonal, D., Buchmann, N., Curtis, P.S., Chen, S., Dong, J., Flanagan, L.B., Frankenberg, C., Georgiadis, T., Gough, C.M., Hui, D., Kiely, G., Li, J., Lund, M., Magliulo, V., Marcolla, B., Merbold, L., Montagnani, L., Moors, E.J., Olesen, J.E., Piao, S., Raschi, A., Roupsard, O., Suyker, A.E., Urbaniak, M., Vaccari, F.P., Varlagin, A., Vesala, T., Wilkinson, M., Weng, E., Wohlfahrt, G., Yan, L., Luo, Y., 2015. Joint control of terrestrial gross primary productivity by plant phenology and physiology. Proc. Natl. Acad. Sci. U. S. A. 112, 2788–2793. https://doi.org/10.1073/pnas.1413090112.

Yan, D., Scott, R.L., Moore, D.J.P., Biederman, J.A., Smith, W.K., 2019. Understanding the relationship between vegetation greenness and productivity across dryland ecosystems through the integration of PhenoCam, satellite, and eddy covariance data. Remote Sens. Environ. 223, 50–62. https://doi.org/10.1016/J.RSE.2018.12.029.

Yang, X., Tang, J., Mustard, J.F., 2014. Beyond leaf color: Comparing camera-based phenological metrics with leaf biochemical, biophysical, and spectral properties throughout the growing season of a temperate deciduous forest. J. Geophys. Res. Biogeosciences 119, 181–191. https://doi.org/10.1002/2013JG002460.

Yang, Y., Ren, W., Tao, B., Ji, L., Liang, L., Ruane, A.C., Fisher, J.B., Liu, J., Sama, M., Li, Z., Tian, Q., 2020. Characterizing spatiotemporal patterns of crop phenology across North America during 2000–2016 using satellite imagery and agricultural survey data. ISPRS J. Photogramm. Remote Sens. 170, 156–173. https://doi.org/10.1016/j.isprsjprs.2020.10.005.

Yao, P., Li, Xiaosha, Nan, W., Li, Xiuyun, Zhang, H., Shen, Y., Li, S., Yue, S., 2017. Carbon dioxide fluxes in soil profiles as affected by maize phenology and nitrogen fertilization in the semiarid Loess Plateau. Agric. Ecosyst. Environ. 236, 120–133. https://doi.org/10.1016/j.agee.2016.11.020.